Satellite Image Segmentation Using Deep Learning for Deforestation Detection

Petro Vorotyntsev
National Technical University of Ukraine "Igor Sikorsky Kyiv Polytechnic Institute"
Kyiv, Ukraine
petervorotyntsev@gmail.com

Yuri Gordienko
National Technical University of Ukraine "Igor Sikorsky Kyiv Polytechnic Institute"
Kyiv, Ukraine
yuri.gordienko@gmail.com

Oleg Alienin
National Technical University of Ukraine "Igor Sikorsky Kyiv Polytechnic Institute"
Kyiv, Ukraine
oleg.alenin@gmail.com

Oleksandr Rokovyi
National Technical University of Ukraine "Igor Sikorsky Kyiv Polytechnic Institute"
Kyiv, Ukraine
alexandr.rokovoy@gmail.com

Sergii Stirenko
National Technical University of Ukraine "Igor Sikorsky Kyiv Polytechnic Institute"
Kyiv, Ukraine
sergii.stirenko@gmail.com

2021 IEEE 3rd Ukraine Conference on Electrical and Computer Engineering (UKRCON) | 978-1-6654-0094-7/21/$31.00 ©2021 IEEE | DOI: 10.1109/UKRCON53503.2021.9575783

***Abstract*—The problem of automatic monitoring the deforestation process is considered for efficient prevention of illegal deforestation. Image segmentation model on the basis of U-Net family of deep neural networks (DNNs) was created. The forest/deforestation dataset was collected by parsing areas of Ukrainian forestries, where satellite images of 512x512 pixels contain areas with forest, deforestation, and other areas. The dataset with satellite imagery and segmented masks was uploaded at GitHub repository where it is available with the correspondent code for distributed training on tensor processing units (TPU). To overcome the imbalance of created dataset the hybrid loss function was created and tested in the training environment. K-fold cross validation and numerous runs for different random seeds were conducted to prove the model and dataset usefulness and stability during the training and validation process. The following asymptotic values of intersection over union (IOU) mean (IOU_{mean}) and standard deviation (IOU_{std}) were obtained after more than 100 epochs: $IOU^{kfold}_{mean} = 0.52, IOU^{kfold}_{std} = 0.03$ for cross-validation, and $IOU^{random}_{mean} = 0.51, IOU^{random}_{std} = 0.03$ for various random seed initialization. These results demonstrate that variation of images in the dataset and randomness of initialization have no significant effect on model performance, but the future research will be needed in the view of the possible increase of datasets where performance could be improved by the larger data representation, but some decrease of performance could be observed due to possible wider data variability. It is especially important for deployment of U-Net-like DNNS on devices with the limited computational resources for Edge Computing layer.**

***Keywords*—deep learning, convolutional neural network, TensorFlow, TPU, image segmentation, U-Net, deforestation**

I. Introduction

Deforestation whether legal or not should be monitored by authorities and it could be difficult to grasp all possible forest cuttings using just the human eye, furthermore the process of counting the area of deforestation by hand from unfiltered satellite imagery is another problem for a human. Regions of illegal deforestation might become unplanted for a long time and reduce the amount of usable tree. Attempts to solve aforesaid problems were attempted in the past [1], [2]. Image thresholding [3] and morphological image transformations [4] were used [1] which were fine for the regions of deforestation visible and understandable for a human eye. For example, the cuttings which were created a few days ago and left the terrain without any vegetation, but such cuttings are just a small percent of all of them. Most of the areas of interest have some amount of vegetation and probably even some amount of newly planted trees, so these areas could not be determined by such methods. Also, the satellite imagery was taken in ultraviolet or infrared spectra which have more information about the amount of vegetation, and tasks of deforestation were solved using the Normalized Difference Vegetation Index (NDVI) [5], [6]. This is an acceptable solution, but usage of open-source satellite imagery with low resolution is not an option in our case, because the area of the forestry sections could be much lower than the resolution of this data. Therefore the dataset was created in the visible range of electromagnetic spectrum. The dataset consists of 322 images, images shape is 512x512 pixels and the dataset is saved in tfrecord format [7]. Tfrecord format was used to increase compatibility with Google Cloud Services. There are, however, a number of obstacles that need to overcome, for example the model predictions are more accurate in the regions which were the most numerous in the dataset distribution. The fact that the dataset for model training was created on the data from Ukrainian forestries means that most of the forest is located on the steppe areas and the terrain of the area was not an important factor for model training. But some areas with special conditions, like forests located on the hill of the mountains, could be

978-1-6654-0094-7/21/$31.00 ©2021 IEEE

completely misclassified due to the shadow of the mountain and predictions are more dependent on the time of the day when satellite images were taken. Also, areas around the forest boundary are the areas of uncertainty for the model. The aforesaid problems could be fixed by a much larger dataset size in comparison to the current size. The main problems for such dataset enlargement are the consistency of labeling rules among all of the images, to prevent ambiguous areas. For example, some areas could look like light deforestation, but some labelers could mark these areas as forest, and the other one as deforestation. These images will make model learning more complicated. The research was done with the model-centric [8] view which declares that the results could become better with more sophisticated model architecture or model's hyperparameters. After satisfactory results with our created U-Net model [9], the dataset was recreated with the data-centric view [8], to further increase the accuracy. The data-centric view declares that the model could not return good results without good data, also known as "garbage in, garbage out". Therefore the dataset was recreated with more precise segmentation.

This paper has the following structure: section *II.Data* contains a brief review of data sources and EDA (Explanatory Data Analysis) [10] of the created dataset, section *III.Methodology* describes the dataset, deep neural networks (DNNs), metrics, and loss function, section *IV.Experimental* gives the results obtained for different DNNs, section *V.Discussion* summarizes all results with analysis of advantages and disadvantages of the methods used, and section *VI.Conclusions and Future Work* outlines the results obtained and propose possible directions for future researches.

II. Data

A. Dataset

Dataset is comprised of 322 pairs of visible spectral images and corresponding masks of shape 512 × 512 × 3. Each image is part of satellite imagery taken over Ukrainian forestries with a view from a height of around 3 kilometres, taken between 2018 and 2021, for a total of 84 million pixels. A low amount of images contain partial cloud cover due to the atmospheric correction. The dataset spans over diverse types of forestries with different terrain what is useful for more solid model training. Table 1 contains the overall amount of segmented pixels per class. 40 pixels were unlabeled during the dataset creation. The distribution of classes in the dataset is imbalanced and this became one of the main training problems.

TABLE I
AMOUNT OF PIXELS PER CLASS

Class	Amount (pixels)
Forest	65196659
Deforestation	9451534
Other	9762135
Total	**84410328**

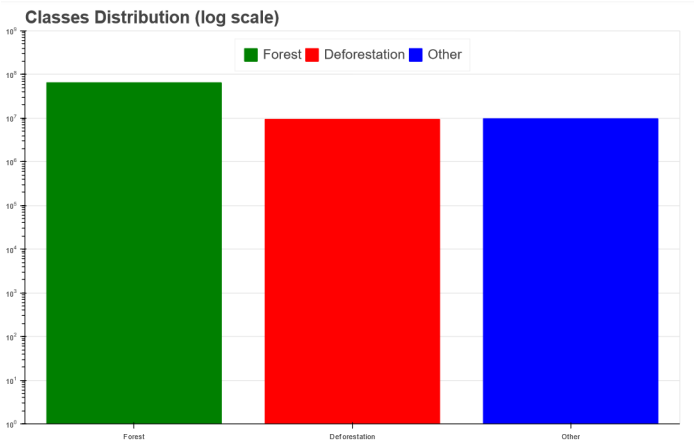

Fig. 1. The log scale distribution shows the total amount of pixels for each class.

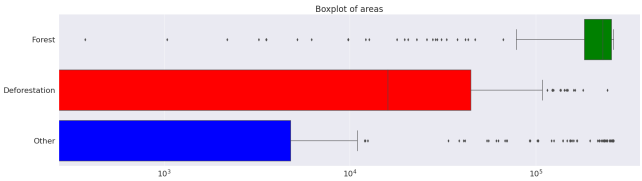

Fig. 2. The boxplot of class areas sizes.

Dataset was created by parsing areas of Ukrainian forestries using PyAutoGui and Google Earth Pro. Images contain not only areas with forest or deforestation, but areas with roads, villages, rivers, and ponds. To make our model more robust and predict areas of deforestation more accurately. The dataset contains masks with three classes: "Forest", "Deforestaion" and "Other". Finally, the dataset with satellite imagery was created for the task considered here and uploaded at GitHub repository[1] where it is available with the correspondent code for distributed training on TPU.

From Fig. 1 it is visible that the amount of pixel from the "Forest" class is one order bigger than the number of pixels in "Deforestation" class, and "Other" class. This means that the model could predict the "Forest" class all the time and get high accuracy.

Fig. 2 shows that for good accuracy, the model should predict very small areas of deforestation. Small areas of forest might be single trees, but it's still important to differentiate them from other classes. The forest area takes 77% taking into account Fig. 3 which means that blind prediction of our model that all pixels belonging to the forest will give it 77% accuracy.

B. Dataset benchmarking

After the creation of the baseline U-Net model [9] for initial predictions, we have segmented the dataset one more time

[1]https://github.com/BioWar/Satellite-Image-Segmentation-using-Deep-Learning-for-Deforestation-Detection

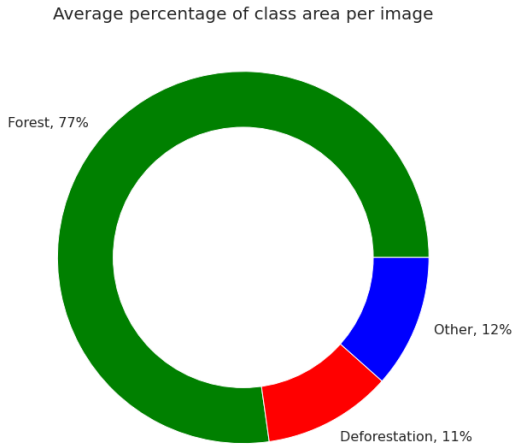

Fig. 3. The average amount of pixels for each class on a single image.

from scratch to create a more accurate one. The second version of the dataset was much better in comparison with the first one, but the problem with both of them is the poor ability to determine the accuracy of the model using such metrics as F1 Score and Intersection over Union (IoU) because the number of minor areas of deforestation and little trees was so huge that it was too work consuming to mark absolutely all of them. Also, no help from subject matter experts was not involved in process of dataset segmentation, so there might be incorrectly labelled areas of deforestation. For example, can we segment the area as deforestation if it contains a certain density of trees and trees of a certain age? This question is hard to answer using satellite imagery.

Example of an image and mask from different versions of the training dataset in Fig. 4. The quality of segmentation on the first mask is lower than on the second one, but the results of model predictions from the initial dataset were still accurate enough.

III. Methodology

A. Loss function

Usage of Categorical Crossentropy [11] loss function gave poor results due to treating all classes equally, but in our case prediction of the "Deforestation" class is the most important. Dice loss and Tversky loss are common choices in image segmentation tasks. Dice loss is a widely used loss function in computer vision. Tversky loss can also be seen as a generalization of the Dices coefficient. It adds weight to false positives and false negatives with the help of coefficients. The idea to combine these loss functions to merge their strengths was taken into account. Therefore loss function similar to the hybrid loss function in AnatomyNet [12] was created and modified to treat the "Deforestation" class as the most valuable by multiplying its contribution to the total loss by a value which would be proportioned to the number of classes the model should predict. Using available data about loss functions for image segmentation [5,6] different combination were checked. The next loss functions was tested: Focal Tversky Loss [13], Dice loss [14], [15], Focal Loss [16], [17], etc. Tversky loss function and Dice loss function were proved to be the best solution for the current problem [18], so they were combined with the factor of lambda for control of the Dice subloss. Focal Tversky Loss not as good as Tversky Loss with manually weighting of class subclasses. Despite on being a good idea to use hybrid loss [12] instead of simple Categorical Crossentropy, the results could be improved much further with a proper new loss function, which will use borders of segmented classes instead of areas [19].

$$TP_p(c) = \sum_{n=1}^{N} p_n(c) g_n(c) \tag{1}$$

$$FN_p(c) = \sum_{n=1}^{N} (1 - p_n(c)) g_n(c) \tag{2}$$

$$FP_p(c) = \sum_{n=1}^{N} p_n(c) (1 - g_n(c)) \tag{3}$$

$$L_{tvsk}(c) = C - \sum_{c=0}^{C-1} w_c \frac{TP_p(c)}{TP_p(c) + \alpha FN_p(c) + \beta FP_p(c)} \tag{4}$$

$$L_{dice}(c) = C - \sum_{c=0}^{C-1} \frac{2 p_n(c) g_n(c) + \epsilon}{p_n(c) + g_n(c) + \epsilon} \tag{5}$$

$$L_{combined} = L_{tvsk} + \lambda * L_{dice} \tag{6}$$

Where TP_p, FN_p and FP_p are the true positives, false negatives and false positives for class c calculated by prediction probabilities respectively, $p_n(c)$ is the predicted probability for pixel n being class c, $g_n(c)$ is the ground truth for pixel n being class c, C is the total number of classes, C=3 in our case, λ is the trade-off between dice loss $L_{dice}(c)$ and tversky loss $L_{tvsk}(c)$, α and β are the trade-offs of penalties for false negatives and false positives which are set to 0.5 in our case, w_c is the weight for class c, in our case weigths for classes "Forest", "Deforestation" and "Other" are equal to 0.4, 2.2 and 0.4 respectively. A high value for the "Deforestation" class is important to overcome the dataset imbalance. Because learning the correct representation of the "Forest" class is the easiest to do.

B. Model

The architecture for the model was chosen to be standard U-Net architecture with the next amount of filters in encoder {32, 64, 128, 256, 512, 1024}, bottleneck with 2048 filters and the decoder part with the same filters as the encoder, starting with 1024, ending with 32. The total amount of trainable parameters is 124,424,995 and equals 475 megabytes of disk space.

Fig. 4. The original satellite imagery (left), the image from the initial dataset (centre), the mask from the final dataset (right).

The RMS-prop optimizer [20] was used with a learning rate equals 1e-6, with other parameters set to their default values. This is the optimal learning rate for this problem, which was proved experimentally, and it helps the model to learn the correct representations of the “Deforestation“ class more accurately. Default learning rate yielded in constant “overshoot” in weights updates.

To speed up training for the model with more than 100 million parameters the distributed TPU (Tensor Processing Unit) [21], [22] strategy was used. Recently, the efficiency of TPU-based training and inference of various DNNs was demonstrated by us on various applications from classification problems [23] (including medical applications [24]) to gesture and pose recognition with the detailed scaling analysis of GPU and TPU performance [25]. Using 8 TPU cores in the Google Colab environment and about 4000 epochs resulted in a clear overfit of the model to training data, but the results of the validation dataset for “Deforestation“ predictions were still acceptable.

IV. Experimental

In this section, the results are presented. The model output is segmented RGB images. Fig. 5 shows the final predictions of the model trained for 4000 epochs. There no major problems with predictions in well visibly demarcated class areas, but there are some bugs with predictions made in the shadow, harsh atmospheric conditions or ploughed fields near the forest. All of the aforesaid areas may be falsely predicted as “Deforestation“. The accuracy of the final model is 95%, taking into account the fact of imbalance in the dataset.

The imbalance of created dataset was overcome by the hybrid loss function described above. K-fold cross validation [26] with k = 6 was conducted at the end of the research to prove the model and dataset usefulness and stability during the training process. Fig. 6 shows the graphics of the k-fold cross-validation of the model. The area filled with colour alongside the average line is the 90% confidence interval. We can conclude that the distribution of images and classes from them

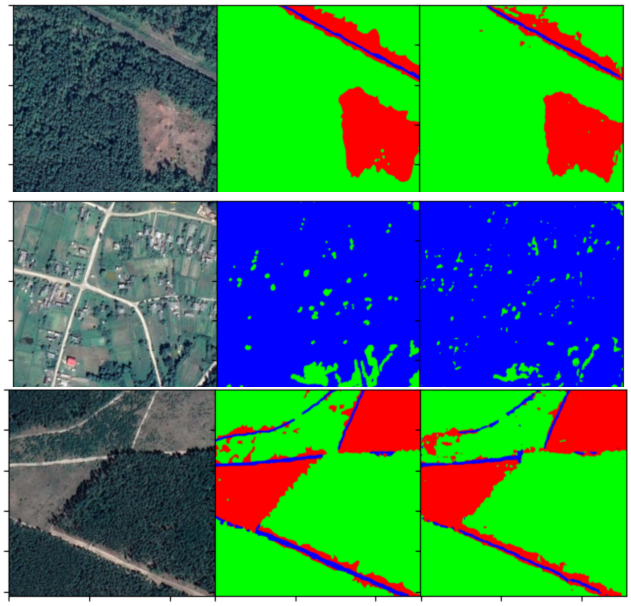

Fig. 5. The original satellite imagery (left), the image from the final dataset (centre), the model prediction (right).

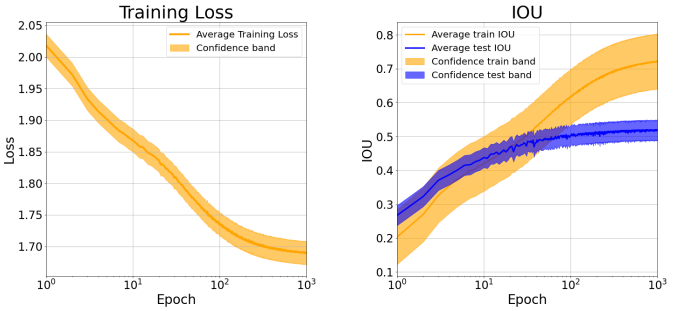

Fig. 6. Graphics of log training loss, and log validation and training IoU for k-fold cross-validation experiment.

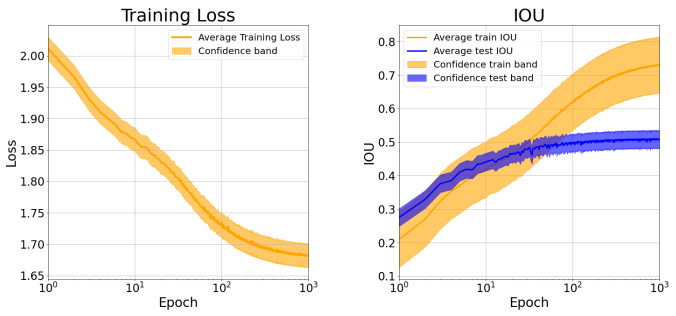

Fig. 7. Graphics of log training loss, and log validation and training IoU for random seeds initialization.

is appropriate enough for the model to learn segmentation rules for this problem. The number of epochs was reduced to 1000 instead of 4000 to obtain results more quickly. Fig. 7 shows the graphics of the random seeds initialization experiment. The following asymptotic values of IOU mean (IOU_{mean}) and standard deviation (IOU_{std}) were obtained after more than 100 epochs: $IOU_{mean}^{kfold} = 0.52, IOU_{std}^{kfold} = 0.03$ for cross-validation (Fig. 6), and $IOU_{mean}^{random} = 0.51, IOU_{std}^{random} = 0.03$ for various random seed initialization (Fig. 7). These results demonstrate that variation of images in the dataset and randomness of initialization have no significant effect on model performance. For further model stability, He normal [27], [28] initialization of convolutional layers was used. The similar approach was applied by us before for medical applications where different effect of data segmentation on the classification performance was observed for small and large datasets [29], [30].

V. Discussion

Model architecture is questionable because it's hard to answer the question: "How deep does the U-Net model have to be to fully meet the accuracy requirements?" Probably results with another couple of millions of trainable parameters would be better, but there is no mathematical derivation of the suitable depth of the model. That's why our model's architecture is more empirically correct than mathematically judging by the final results. The same questions about the model architecture and performance were raised in [31] and the conclusion was that family of U-Net models have reached their peak, and to obtain more precise results new architecture are required like [32], [33]. The similar approach was successfully used by us before for several medical applications where semantic segmentation tasks should be resolved and compromise between the training duration and performance should be found for the small available medical datasets [34], [35].

In the more general context the future investigation of the smaller U-Net DNNs could be very promising for their deployment on TPU-based devices with the limited computational resources for Edge Computing layer [36], [37]. That is why the additional research to find compromise between accuracy and speed should be determined for the specific Edge Computing device and application demands [36], [38]. Also, the possible increase of the dataset could result in improvement of model performance, but some decrease of performance could be observed due to possible wider data variablity in the updated dataset.

VI. Conclusions

The results obtained allowed us to conclude that the problem of automatic monitoring the deforestation process for efficient prevention of illegal deforestation can be efficiently resolved by the method proposed. Despite the limited number of satellite images in the considered dataset, the proposed image segmentation model on the basis of U-Net family achieved the reasonable results with the strictly defined segmentation metrics with mean and standard deviation values measured by k-fold cross validation and numerous runs for different random seeds. The dataset with satellite imagery and segmented masks was uploaded at GitHub repository and could be increased by size and variety of data to check the correspondent influence. It should be emphasized that these training/validation methods and segmentation results obtained can be used in the more general context (and they are actually used for the medical applications mentioned above), but the more extended research will be necessary, especially for deployment of the U-Net DNNs on Edge Computing TPU-based devices with the limited computational resources for the aforementioned applications.

Acknowledgment

The work was partially supported by the National Research Foundation of Ukraine by the grant 2020.01/0490 "Artificial Intelligence Platform for Distant Computer-Aided Detection (CADe) and Computer-Aided Diagnosis (CADx) of Human Diseases".

References

[1] Margono, B. A., Turubanova, S., Zhuravleva, I., Potapov, P., Tyukavina, A., Baccini, A., ... & Hansen, M. C. (2012). Mapping and monitoring deforestation and forest degradation in Sumatra (Indonesia) using Landsat time series data sets from 1990 to 2010. Environmental Research Letters, 7(3), 034010.

[2] Pereira, G. H. D. A., Fusioka, A. M., Nassu, B. T., & Minetto, R. (2021). Active Fire Detection in Landsat-8 Imagery: a Large-Scale Dataset and a Deep-Learning Study. arXiv preprint arXiv:2101.03409.

[3] Barron, J. T. (2020, August). A Generalization of Otsu's Method and Minimum Error Thresholding. In European Conference on Computer Vision (pp. 455-470). Springer, Cham.

[4] Sreedhar, K., & Panlal, B. (2012). Enhancement of images using morphological transformation. arXiv preprint arXiv:1203.2514.

[5] Tucker, C. J. (1979). Red and photographic infrared linear combinations for monitoring vegetation. Remote sensing of Environment, 8(2), 127-150.

[6] Rouse, J. W., Haas, R. H., Schell, J. A., & Deering, D. W. (1974). Monitoring vegetation systems in the Great Plains with ERTS. NASA special publication, 351(1974), 309.

[7] Aizman, A., Maltby, G., & Breuel, T. (2019, December). High Performance I/O For Large Scale Deep Learning. In 2019 IEEE International Conference on Big Data (Big Data) (pp. 5965-5967). IEEE.

[8] Bossér, J. D., Sörstadius, E., & Chehreghani, M. H. (2020). Model-Centric and Data-Centric Aspects of Active Learning for Neural Network Models. arXiv preprint arXiv:2009.10835.

[9] Ronneberger, O., Fischer, P., & Brox, T. (2015, October). U-net: Convolutional networks for biomedical image segmentation. In International Conference on Medical image computing and computer-assisted intervention (pp. 234-241). Springer, Cham.

[10] Wongsuphasawat, K., Liu, Y., & Heer, J. (2019). Goals, process, and challenges of exploratory data analysis: an interview study. arXiv preprint arXiv:1911.00568.

[11] Murphy, K. P. (2012). Machine learning: a probabilistic perspective. MIT press.

[12] Zhu, W., Huang, Y., Zeng, L., Chen, X., Liu, Y., Qian, Z., ... & Xie, X. (2019). AnatomyNet: Deep learning for fast and fully automated whole-volume segmentation of head and neck anatomy. Medical physics, 46(2), 576-589.

[13] Salehi, S. S. M., Erdogmus, D., & Gholipour, A. (2017, September). Tversky loss function for image segmentation using 3D fully convolutional deep networks. In International workshop on machine learning in medical imaging (pp. 379-387). Springer, Cham.

[14] Li, X., Sun, X., Meng, Y., Liang, J., Wu, F., & Li, J. (2019). Dice loss for data-imbalanced NLP tasks. arXiv preprint arXiv:1911.02855.

[15] Bertels, J., Eelbode, T., Berman, M., Vandermeulen, D., Maes, F., Bisschops, R., & Blaschko, M. B. (2019, October). Optimizing the dice score and jaccard index for medical image segmentation: Theory and practice. In International Conference on Medical Image Computing and Computer-Assisted Intervention (pp. 92-100). Springer, Cham.

[16] Lin, T. Y., Goyal, P., Girshick, R., He, K., & Dollár, P. (2017). Focal loss for dense object detection. In Proceedings of the IEEE international conference on computer vision (pp. 2980-2988).

[17] Li, X., Wang, W., Wu, L., Chen, S., Hu, X., Li, J., ... & Yang, J. (2020). Generalized focal loss: Learning qualified and distributed bounding boxes for dense object detection. arXiv preprint arXiv:2006.04388.

[18] Jadon, S. (2020, October). A survey of loss functions for semantic segmentation. In 2020 IEEE Conference on Computational Intelligence in Bioinformatics and Computational Biology (CIBCB) (pp. 1-7). IEEE.

[19] Kervadec, H., Bouchtiba, J., Desrosiers, C., Granger, E., Dolz, J., & Ayed, I. B. (2019, May). Boundary loss for highly unbalanced segmentation. In International conference on medical imaging with deep learning (pp. 285-296). PMLR.

[20] De, S., Mukherjee, A., & Ullah, E. (2018). Convergence guarantees for RMSProp and ADAM in non-convex optimization and an empirical comparison to Nesterov acceleration. arXiv preprint arXiv:1807.06766.

[21] Wang, Y. E., Wei, G. Y., & Brooks, D. (2019). Benchmarking tpu, gpu, and cpu platforms for deep learning. arXiv preprint arXiv:1907.10701.

[22] Jouppi, N. P., Young, C., Patil, N., Patterson, D., Agrawal, G., Bajwa, R., ... & Yoon, D. H. (2017, June). In-datacenter performance analysis of a tensor processing unit. In Proceedings of the 44th annual international symposium on computer architecture (pp. 1-12).

[23] Kochura, Y., Gordienko, Y., Taran, V., Gordienko, N., Rokovyi, A., Alienin, O., Stirenko, S., Batch size influence on performance of graphic and tensor processing units during training and inference phases. In International Conference on Computer Science, Engineering and Education Applications (658-668). Springer, Cham, 2019.

[24] Doms, V., Yuri Gordienko, Yuriy Kochura, Oleksandr Rokovyi, Oleg Alienin, and Sergii Stirenko, Deep Learning for Melanoma Detection with Testing Time Data Augmentation, Proceeedings of The First International Conference on Artificial Intelligence and Logistics Engineering (January 22 - January 24, 2021), Kyiv, Ukraine, 2021.

[25] Gordienko, Y., Kochura, Y., Taran, V., Gordienko, N., Rokovyi, A., Alienin, O., Stirenko, S., Scaling Analysis of Specialized Tensor Processing Architectures for Deep Learning Models. In Deep Learning: Concepts and Architectures (65-99). Springer, Cham, 2020.

[26] Kohavi, R. (1995, August). A study of cross-validation and bootstrap for accuracy estimation and model selection. In Ijcai (Vol. 14, No. 2, pp. 1137-1145).

[27] Glorot, X., Bordes, A., & Bengio, Y. (2011, June). Deep sparse rectifier neural networks. In Proceedings of the fourteenth international conference on artificial intelligence and statistics (pp. 315-323). JMLR Workshop and Conference Proceedings.

[28] He, K., Zhang, X., Ren, S., & Sun, J. (2015). Delving deep into rectifiers: Surpassing human-level performance on imagenet classification. In Proceedings of the IEEE international conference on computer vision (pp. 1026-1034).

[29] Gang, P., Zeng, W., Gordienko, Y., Kochura, Y., Alienin, O., Rokovyi, O., & Stirenko, S., Effect of Data Augmentation and Lung Mask Segmentation for Automated Chest Radiograph Interpretation of Some Lung Diseases. In International Conference on Neural Information Processing, Springer, Cham, pp. 333-340, 2019.

[30] Gordienko, Y., Gang, P., Hui, J., Zeng, W., Kochura, Y., Alienin, O., ... & Stirenko, S. (2018, January). Deep learning with lung segmentation and bone shadow exclusion techniques for chest X-ray analysis of lung cancer. In International Conference on Computer Science, Engineering and Education Applications (pp. 638-647). Springer, Cham.

[31] Roman Statkevych, Sergii Stirenko, Yuri Gordienko (2020). Human Kidney Tissue Image Segmentation by U-Net Models (submitted)

[32] Zhou, C., Ding, C., Wang, X., Lu, Z., & Tao, D. (2020). One-pass multi-task networks with cross-task guided attention for brain tumor segmentation. IEEE Transactions on Image Processing, 29, 4516-4529.

[33] Huang, C. H., Wu, H. Y., & Lin, Y. L. (2021). HarDNet-MSEG: A Simple Encoder-Decoder Polyp Segmentation Neural Network that Achieves over 0.9 Mean Dice and 86 FPS. arXiv preprint arXiv:2101.07172.

[34] Stirenko, S., Kochura, Y., Alienin, O., Rokovyi, O., Gordienko, Y., Gang, P., & Zeng, W. (2018, April). Chest X-ray analysis of tuberculosis by deep learning with segmentation and augmentation. In 2018 IEEE 38th International Conference on Electronics and Nanotechnology (ELNANO) (pp. 422-428). IEEE.

[35] Yu. Gordienko, Yu. Kochura, O. Alienin, O. Rokovyi, S. Stirenko, Peng Gang, Jiang Hui, Wei Zeng (2018) Dimensionality Reduction in Deep Learning for Chest X-Ray Analysis of Lung Cancer, Proceedings of 10th International Conference on Advanced Computational Intelligence (ICACI-2018), IEEE, pp. 878-883, 2018.

[36] Cao, K., Liu, Y., Meng, G., Sun, Q, An Overview on Edge Computing Research. IEEE Access, 8, 85714-85728, 2020.

[37] Gordienko, Y., et al, Augmented coaching ecosystem for non-obtrusive adaptive personalized elderly care on the basis of Cloud-Fog-Dew computing paradigm. In 2017 40th International Convention on Information and Communication Technology, Electronics and Microelectronics (MIPRO) (359-364). IEEE, 2017.

[38] Gordienko, Y., Kochura, Y., Taran, V., Gordienko, N., Rokovyi, O., Alienin, O., Stirenko, S., Last mile optimization of edge computing ecosystem with deep learning models and specialized tensor processing architectures, Advances in Computers, Elsevier, doi: 10.1016/bs.adcom.2020.10.003, 2020.